QCD equation of state at finite baryon density with fugacity expansion

Volodymyr Vovchenko

Goethe University Frankfurt & Frankfurt Institute for Advanced Studies

$$\frac{p(T,\mu_B)}{T^4} = \sum_{k=0}^{\infty} p_k(T) \cosh\left(\frac{k\,\mu_B}{T}\right)$$

V.V., J. Steinheimer, O. Philipsen, H. Stoecker, PRD 97, 114030 (2018), *work in progress*

CPOD 2018, Corfu, Greece

September 28, 2018

QCD phase diagram: towards finite density

?

$\mu_B = 0$ → $T - \mu_B$ plane

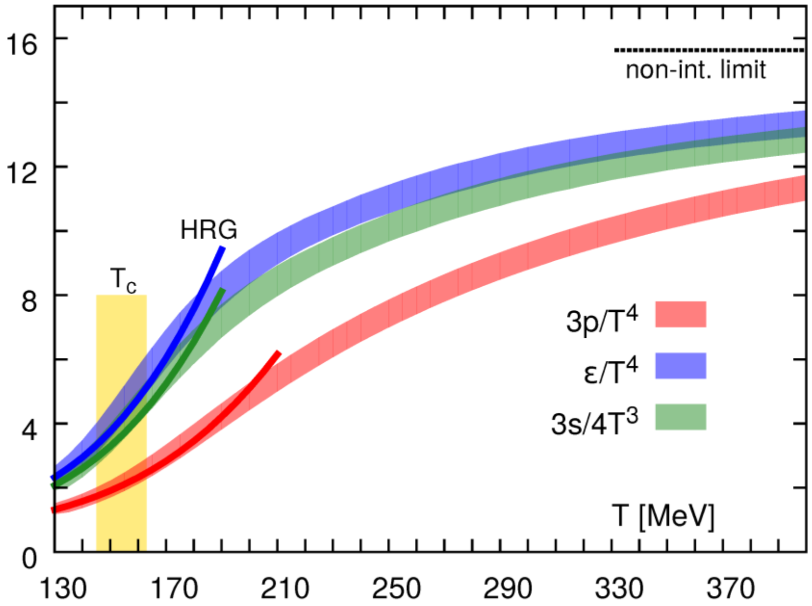

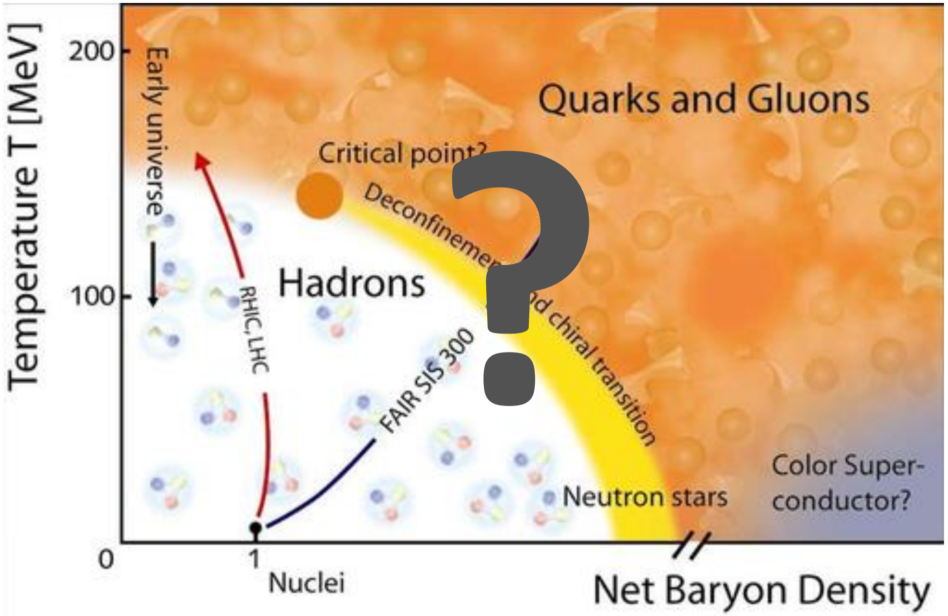

- QCD equation of state at $\mu_B = 0$ available from lattice QCD
- No direct LQCD simulations at finite μ_B but recently a lot of LQCD data which helps constrain/formulate phenomenological models

QCD thermodynamics with fugacity expansion

$$\frac{p(T,\mu_B)}{T^4} = \sum_{k=0}^{\infty} p_k(T)\,\cosh\left(\frac{k\,\mu_B}{T}\right) = \sum_{k=-\infty}^{\infty} \tilde{p}_{|k|}(T)\, e^{k\mu_B/T}$$

No sign problem on the lattice at imaginary $\mu_B \to i\tilde{\mu}_B$

Observables obtain trigonometric Fourier series form

Baryon density: $\frac{\rho_B(T,\mathrm{i}\tilde{\mu}_B)}{T^3} = \mathrm{i}\sum_{k=1}^{\infty} b_k(T)\,\sin\left(\frac{k\,\tilde{\mu}_B}{T}\right), \quad b_k(T) \equiv k\,p_k(T)$

$$b_k(T) = \frac{2}{\pi\,T^4}\int_0^{\pi T} d\tilde{\mu}_B\,[\mathrm{Im}\,\rho_B(T,i\tilde{\mu}_B)]\,\sin(k\,\tilde{\mu}_B/T)$$

QCD thermodynamics with fugacity expansion

$$\frac{p(T,\mu_B)}{T^4} = \sum_{k=0}^{\infty} p_k(T) \cosh\left(\frac{k\,\mu_B}{T}\right) = \sum_{k=-\infty}^{\infty} \tilde{p}_{|k|}(T)\, e^{k\mu_B/T}$$

No sign problem on the lattice at imaginary $\mu_B \to i\tilde{\mu}_B$

Observables obtain trigonometric Fourier series form

Baryon density: $\frac{\rho_B(T, \mathrm{i}\tilde{\mu}_B)}{T^3} = \mathrm{i} \sum_{k=1}^{\infty} b_k(T) \sin\left(\frac{k\,\tilde{\mu}_B}{T}\right), \quad b_k(T) \equiv k\, p_k(T)$

$$b_k(T) = \frac{2}{\pi\, T^4} \int_0^{\pi T} d\tilde{\mu}_B \,[\mathrm{Im}\,\rho_B(T, i\tilde{\mu}_B)]\, \sin(k\,\tilde{\mu}_B/T)$$

Ideal (Boltzmann) HRG:

$$\frac{\rho_B}{T^3} = b_1(T)\sinh\left(\frac{\mu_B}{T}\right)$$

Massless quarks (Stefan-Boltzmann limit):

$$b_k^{\mathrm{SB}} = \frac{(-1)^{k+1}}{k}\,\frac{4\,[3+4\,(\pi k)^2]}{27\,(\pi k)^2}$$

Lattice QCD results on Fourier coefficients

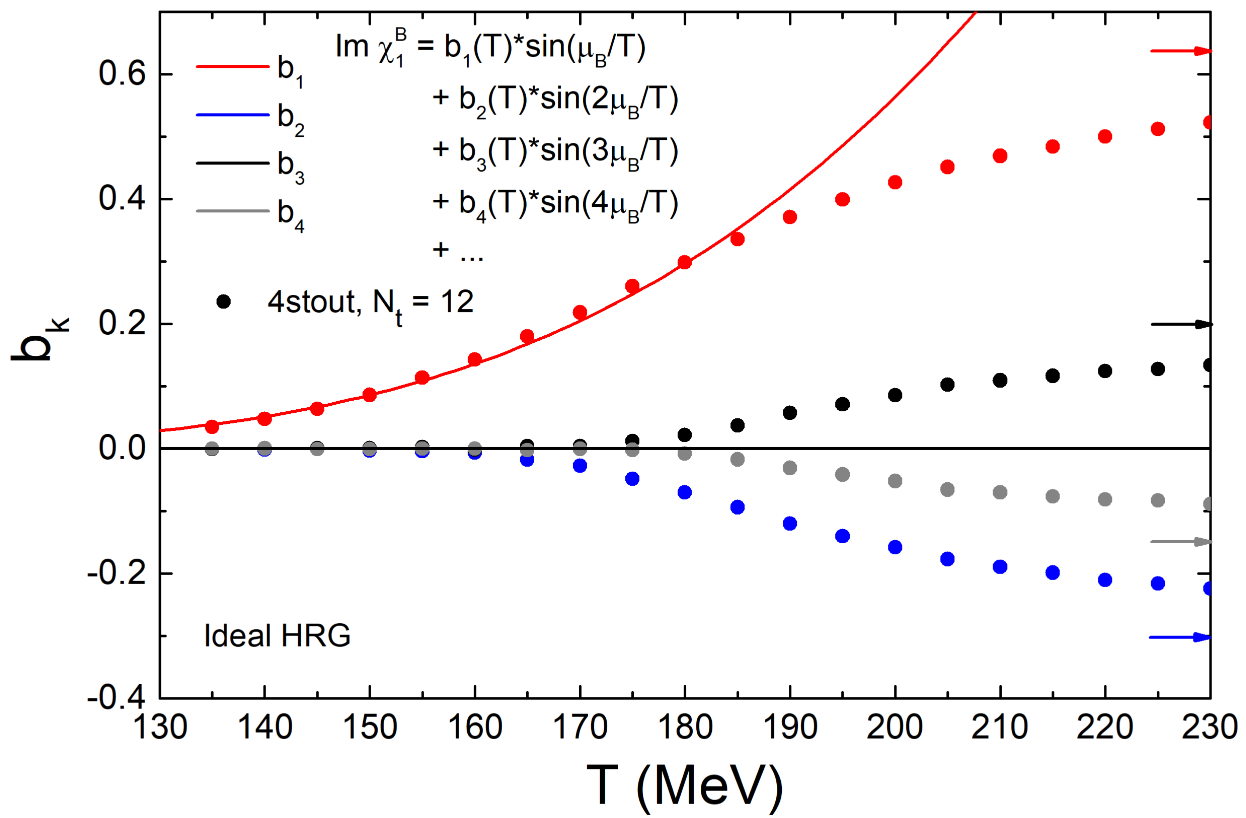

S. Borsanyi et al. [Wuppertal-Budapest collaboration], QM2017

- Consistent with HRG at low temperatures
- Consistent with approach to the Stefan-Boltzmann limit
- b_2 visibly departs from zero above $T \sim 160$ MeV

HRG with repulsive baryonic interactions

Repulsive interactions with excluded volume (EV) $V \to V - bN$

[Hagedorn, Rafelski, ’80; Dixit, Karsch, Satz, ’81; Cleymans et al., ‘86; Rischke et al., Z. Phys. C ‘91]

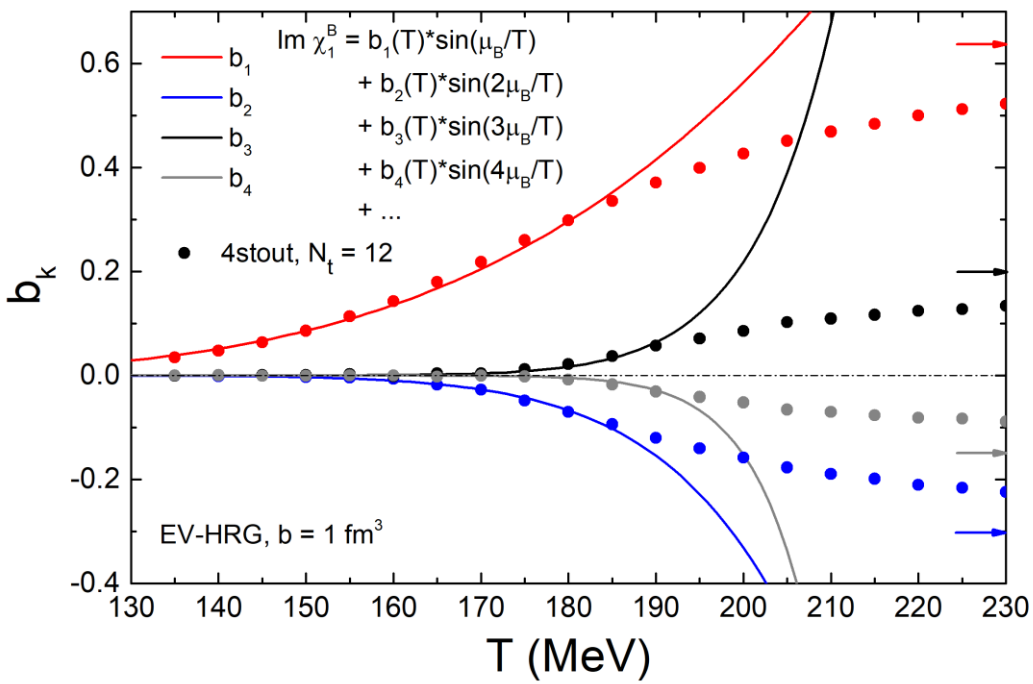

HRG with baryonic EV:

$$p_B(T,\mu_B) = p_B^{\rm id}(T,\mu_B - b p_B)$$

$$b_k^{ev}(T) = (-1)^{k-1} \frac{2\,k^k}{k!} (b\,T^3)^{k-1} \left[\frac{\phi_B(T)}{T^3}\right]^k$$

V.V., A. Pasztor, Z. Fodor,
S.D. Katz, H. Stoecker, 1708.02852

- Non-zero $b_k(T)$ for $k \geq 2$ signal deviation from ideal HRG
- EV interactions between baryons ($b \approx 1$ fm^3) reproduce lattice trend

EV-HRG: (cross-)susceptibilities

Comparison with LQCD data from F. Karsch's talk on Tuesday

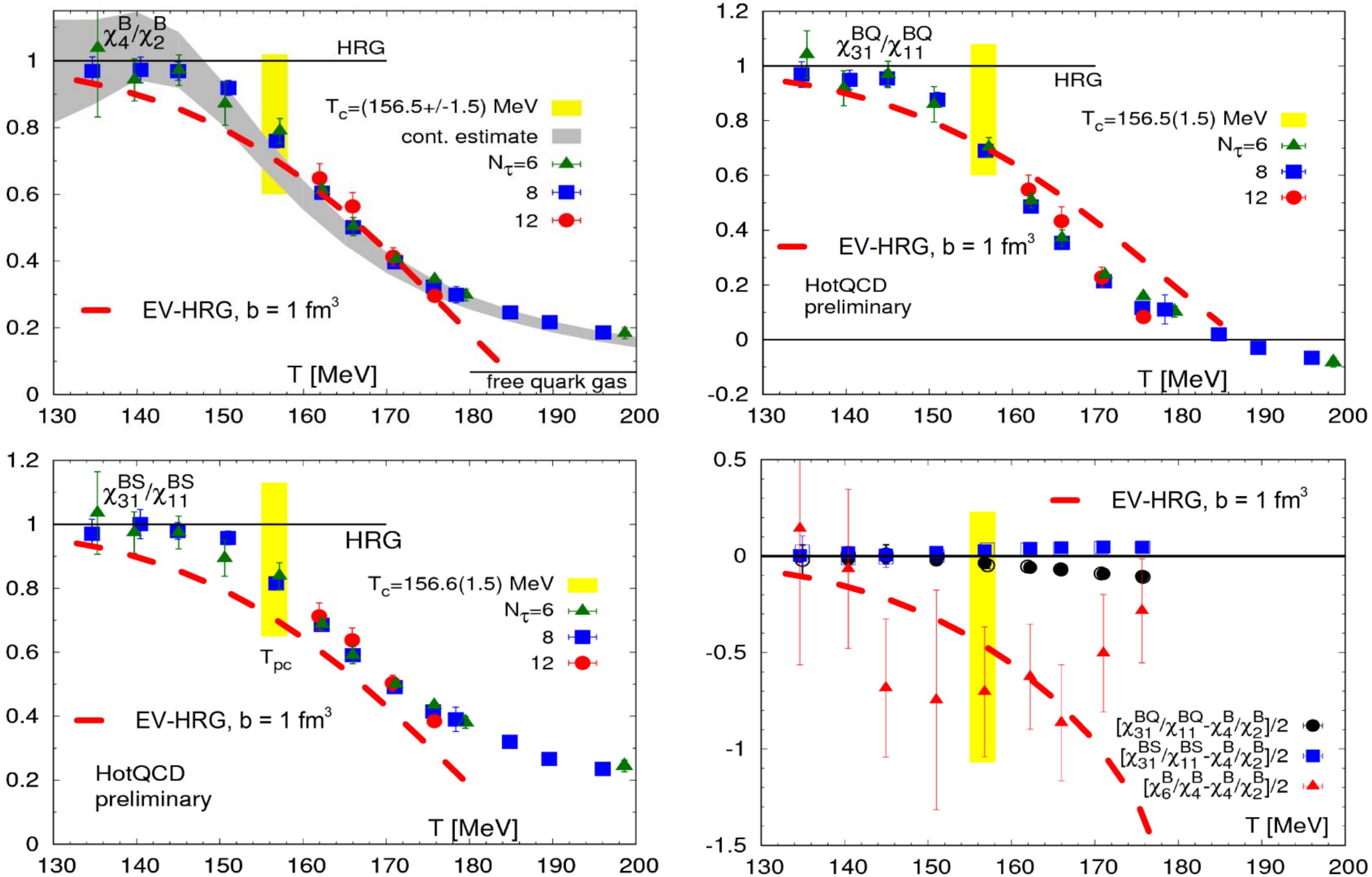

Higher-order coefficients from lower ones

Feature of the EV-like models: temperature-independent ratios

$$\alpha_3 = \frac{b_1(T)}{[b_2(T)]^2} b_3(T), \qquad \alpha_4 = \frac{[b_1(T)]^2}{[b_2(T)]^3} b_4(T), \quad \ldots \quad \alpha_k = \frac{[b_1(T)]^{k-2}}{[b_2(T)]^{k-1}} b_k(T)$$

Higher-order coefficients from lower ones

Feature of the EV-like models: temperature-independent ratios

$$\alpha_3 = \frac{b_1(T)}{[b_2(T)]^2} b_3(T), \qquad \alpha_4 = \frac{[b_1(T)]^2}{[b_2(T)]^3} b_4(T), \quad \ldots \quad \alpha_k = \frac{[b_1(T)]^{k-2}}{[b_2(T)]^{k-1}} b_k(T)$$

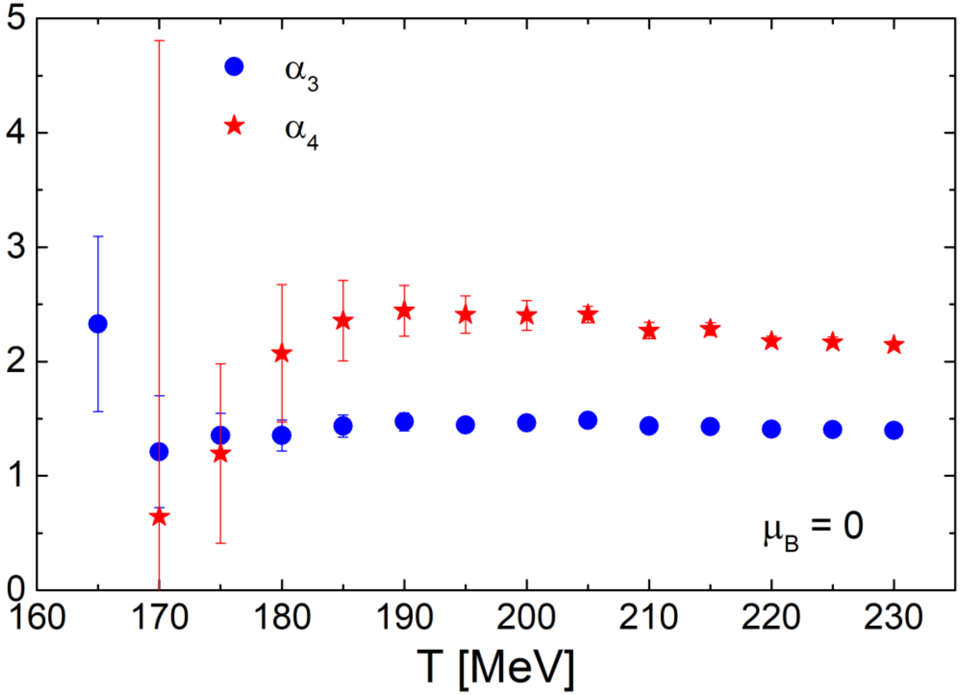

Observation: α_3 and α_4 are *T*-independent in lattice data

Higher-order coefficients from lower ones

Feature of the EV-like models: temperature-independent ratios

$$\alpha_3 = \frac{b_1(T)}{[b_2(T)]^2} b_3(T), \qquad \alpha_4 = \frac{[b_1(T)]^2}{[b_2(T)]^3} b_4(T), \quad \ldots \quad \alpha_k = \frac{[b_1(T)]^{k-2}}{[b_2(T)]^{k-1}} b_k(T)$$

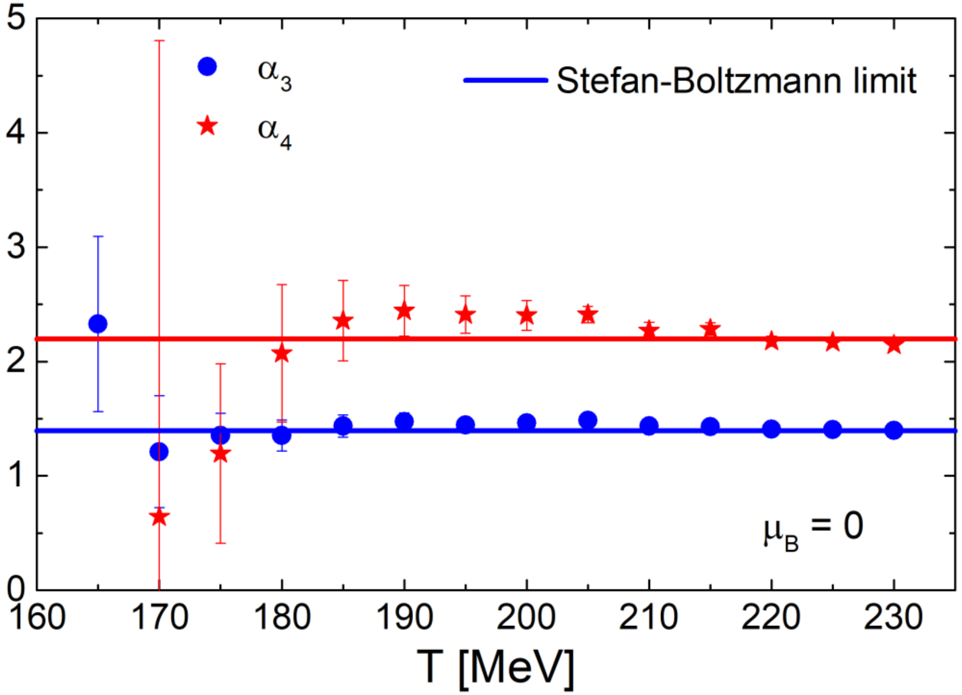

Stefan-Boltzmann limit:

$$\alpha_k^{SB} = 8^{k-1} \frac{(3+4\pi^2)^{k-2}}{(3+16\pi^2)^{k-1}} \frac{3+4\pi^2 k^2}{k^3}$$

$\alpha_4^{SB} \cong 2.198$

$\alpha_3^{SB} \cong 1.394$

Observation: α_3 and α_4 are T-independent in lattice data

Ratios are consistent with Stefan-Boltzmann limit of massless quarks

Cluster Expansion Model — CEM

a model for QCD equation of state at finite baryon density

V. Vovchenko, J. Steinheimer, O. Philipsen, H. Stoecker, 1711.01261, work in progress

Cluster Expansion Model (CEM)

Model formulation:

- Fugacity expansion for baryon number density

$$\frac{\rho_B(T,\mu_B)}{T^3} = \chi_1^B(T,\mu_B) = \sum_{k=1}^{\infty} b_k(T)\,\sinh(k\mu_B/T)$$

- $b_1(T)$ and $b_2(T)$ are model input
- All higher order coefficients are predicted: $b_k(T) = \alpha_k^{SB} \frac{[b_2(T)]^{k-1}}{[b_1(T)]^{k-2}}$

Physical picture: Hadron gas with repulsion at moderate *T*, "weakly" interacting quarks and gluons at high *T*

Cluster Expansion Model (CEM)

Model formulation:

- Fugacity expansion for baryon number density

$$\frac{\rho_B(T,\mu_B)}{T^3} = \chi_1^B(T,\mu_B) = \sum_{k=1}^{\infty} b_k(T) \sinh(k\mu_B/T)$$

- $b_1(T)$ and $b_2(T)$ are model input
- All higher order coefficients are predicted: $b_k(T) = \alpha_k^{SB} \frac{[b_2(T)]^{k-1}}{[b_1(T)]^{k-2}}$

Physical picture: Hadron gas with repulsion at moderate *T*, "weakly" interacting quarks and gluons at high *T*

Summed analytic form:

$$\frac{\rho_B(T,\mu_B)}{T^3} = -\frac{2}{27\pi^2}\frac{\hat{b}_1^2}{\hat{b}_2}\left\{4\pi^2\left[\mathrm{Li}_1(x_+) - \mathrm{Li}_1(x_-)\right] + 3\left[\mathrm{Li}_3(x_+) - \mathrm{Li}_3(x_-)\right]\right\}$$

$$\hat{b}_{1,2} = \frac{b_{1,2}(T)}{b_{1,2}^{\mathrm{SB}}}, \quad x_\pm = -\frac{\hat{b}_2}{\hat{b}_1} e^{\pm\mu_B/T}, \quad \mathrm{Li}_s(z) = \sum_{k=1}^{\infty} \frac{z^k}{k^s}$$

Regular behavior at real μ_B → *no-critical-point scenario*

CEM: Baryon number susceptibilities

$$\chi_k^B(T,\mu_B) = -\frac{2}{27\pi^2}\frac{\hat{b}_1^2}{\hat{b}_2}\left\{4\pi^2\left[\mathrm{Li}_{2\text{-k}}(x_+) + (-1)^k\ \mathrm{Li}_{2\text{-k}}(x_-)\right] + 3\left[\mathrm{Li}_{4\text{-k}}(x_+) + (-1)^k\ \mathrm{Li}_{4\text{-k}}(x_-)\right]\right\}$$

CEM-LQCD: $b_1(T)$ and $b_2(T)$ from LQCD simulations at imaginary μ_B

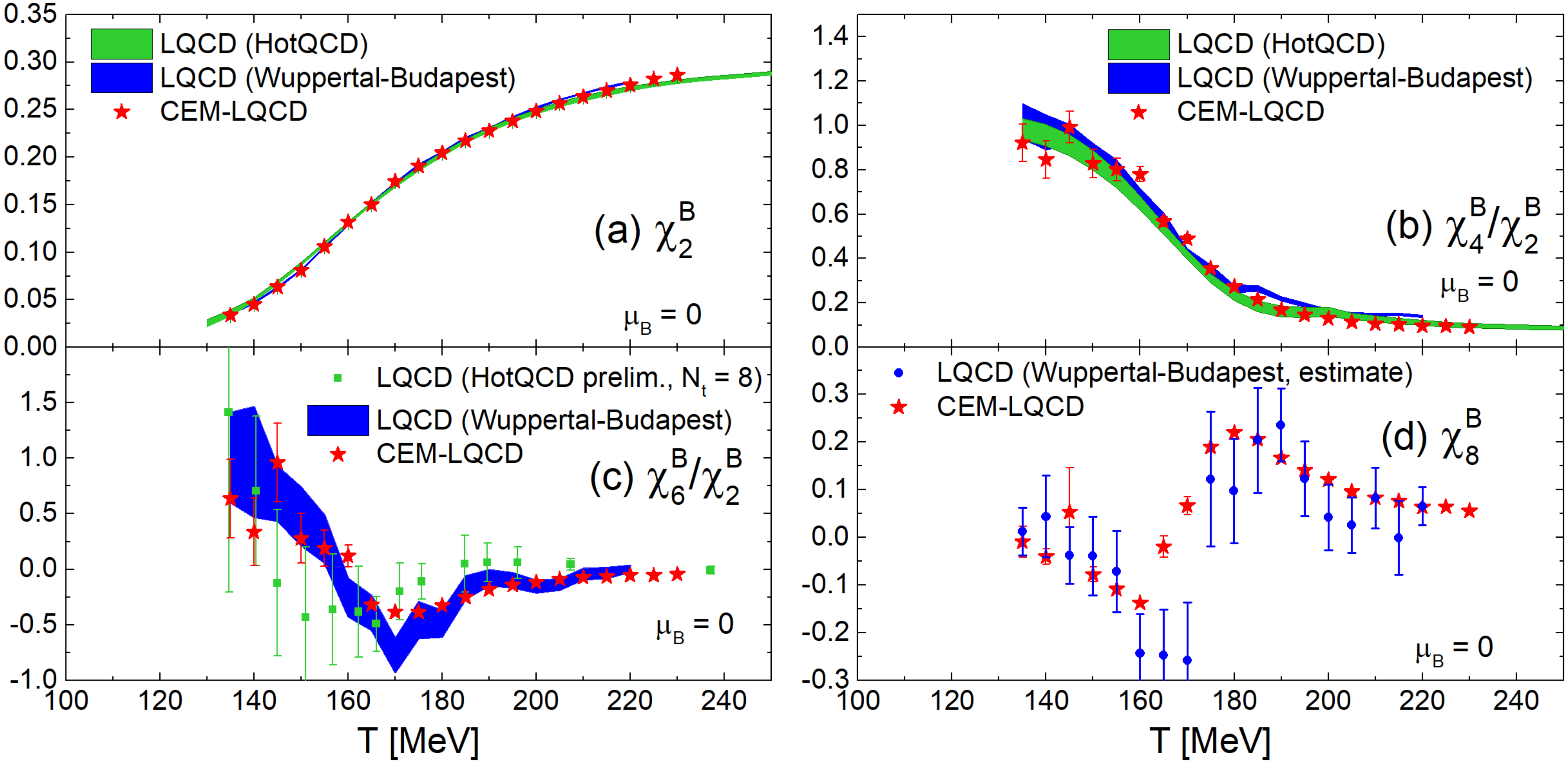

Lattice data from 1805.04445 (Wuppertal-Budapest), 1701.04325 & 1708.04897 (HotQCD)

Non-uniqueness of the recursion relation

Defining $b_k(T)$ from $b_1(T)$ and $b_2(T)$ is not unique

Rational function model (RFM): G. Almasi, B. Friman, K. Morita, P. Lo, K. Redlich, 1805.04441

$$b_k^{RMF}(T) = \frac{c(T)}{1+\sqrt{k^2}/k_0(T)}\, b_k^{SB}, \quad k_0(T) = \left[\frac{\hat{b}_1(T)}{\hat{b}_2(T)} - 1\right]^{-1} - 1, \quad c(T) = \hat{b}_1(T)\left(1 + \frac{1}{k_0(T)}\right)$$

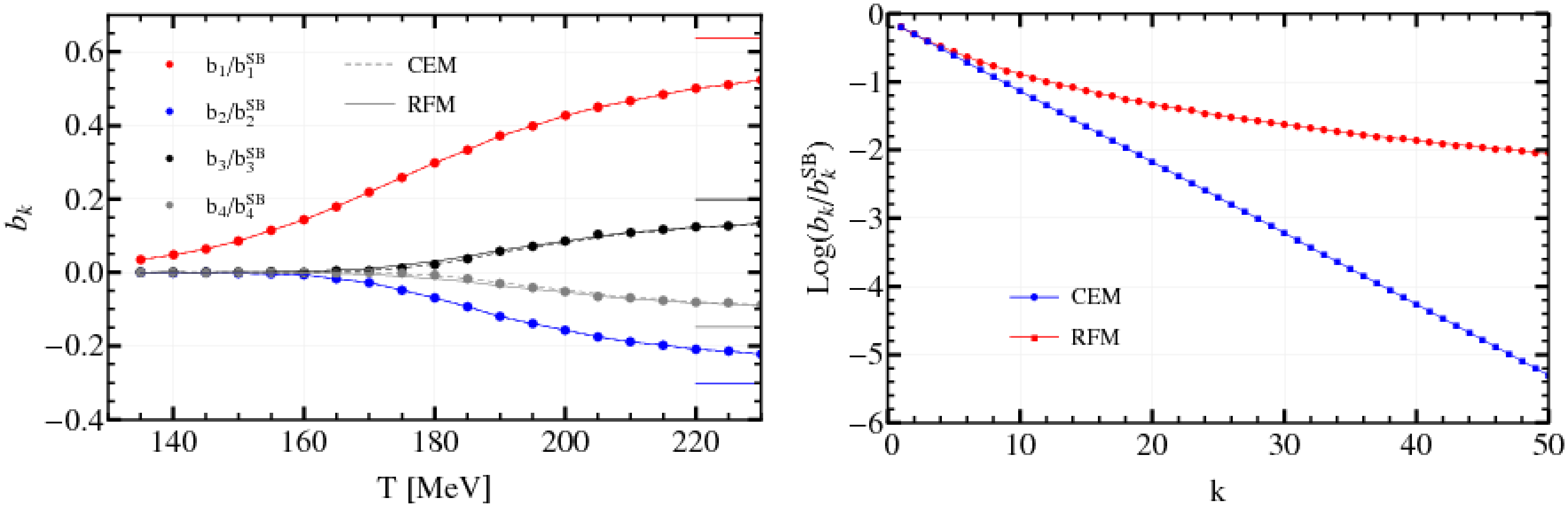

CEM and RFM yield comparable predictions for $b_3(T)$ and $b_4(T)$ but very different asymptotic behavior

CEM vs RFM: Susceptibilities

$$\chi_n^B = \sum_{k=1}^{\infty} k^n\, b_k(T) = b_1(T) + 2^n b_2(T) + 3^n b_3(T) + 4^n b_4(T) + \cdots$$

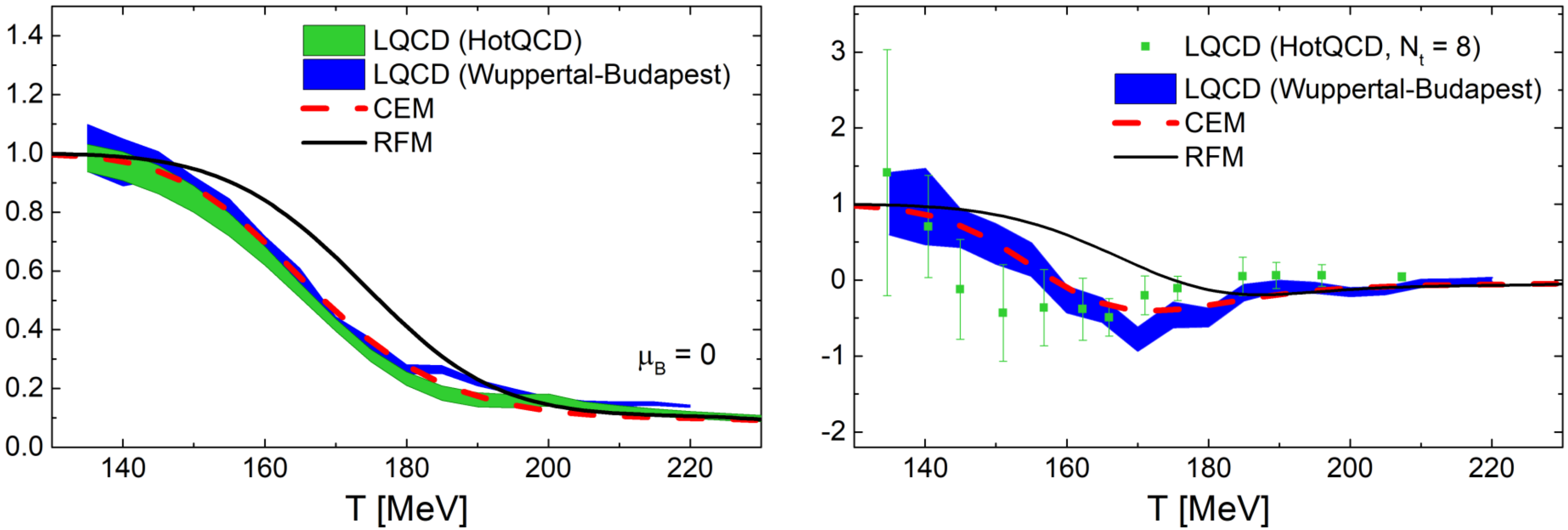

Lattice data at $\mu_B = 0$ can distinguish models that are difficult to separate with data at imaginary μ_B

Important to incorporate constraints from

both imaginary μ_B and $\mu_B = 0$

Radius of convergence

Taylor expansion of the QCD pressure:

$$\frac{p(T,\mu_B)}{T^4} = \frac{p(T,0)}{T^4} + \frac{\chi_2^B(T)}{2!}(\mu_B/T)^2 + \frac{\chi_4^B(T)}{4!}(\mu_B/T)^4 + \ldots$$

Radius of convergence $r_{\mu/T}$ of the expansion is the distance to the nearest singularity of p/T^4 in the complex μ_B/T plane, which could point to the QCD critical point

Lattice QCD strategy: Estimate $r_{\mu/T}$ from few leading terms

[M. D'Elia et al., 1611.08285; S. Datta et al., 1612.06673; A. Bazavov et al., 1701.04325]

Radius of convergence

Taylor expansion of the QCD pressure:

$$\frac{p(T,\mu_B)}{T^4} = \frac{p(T,0)}{T^4} + \frac{\chi_2^B(T)}{2!}(\mu_B/T)^2 + \frac{\chi_4^B(T)}{4!}(\mu_B/T)^4 + \dots$$

Radius of convergence $r_{\mu/T}$ of the expansion is the distance to the nearest singularity of p/T^4 in the complex μ_B/T plane, which could point to the QCD critical point

Lattice QCD strategy: Estimate $r_{\mu/T}$ from few leading terms

[M. D'Elia et al., 1611.08285; S. Datta et al., 1612.06673; A. Bazavov et al., 1701.04325]

CEM: $\chi_1^B \propto \mathrm{Li}\left(-\frac{\hat{b}_2}{\hat{b}_1} e^{\mu_B/T}\right) \quad \Rightarrow \quad (\mu_B/T)_c = \pm \ln\left(\frac{\hat{b}_1}{\hat{b}_2}\right) \pm i\,\pi$

Singularity in the *complex plane* → what are the *consequences?*

CEM: Structure of Taylor coefficients

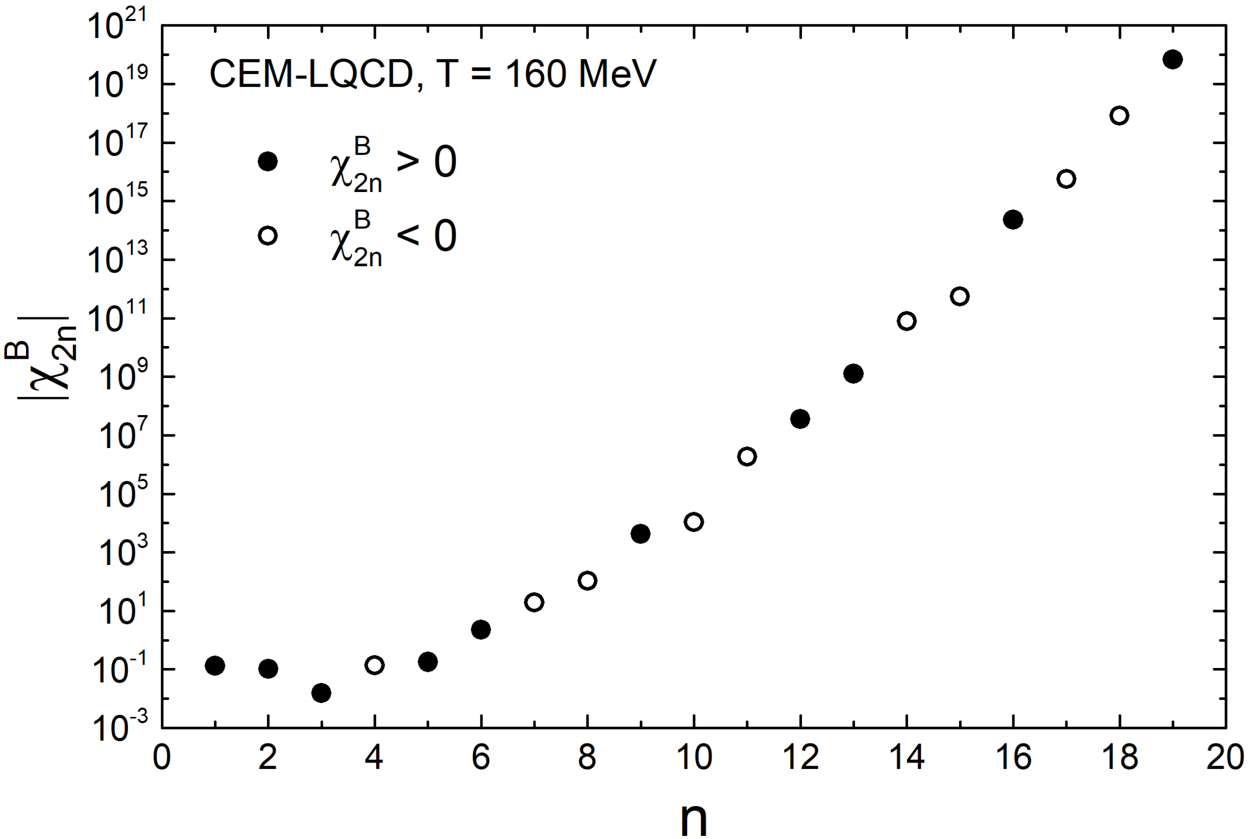

Negative coefficients appear eventually

CEM: Structure of Taylor coefficients

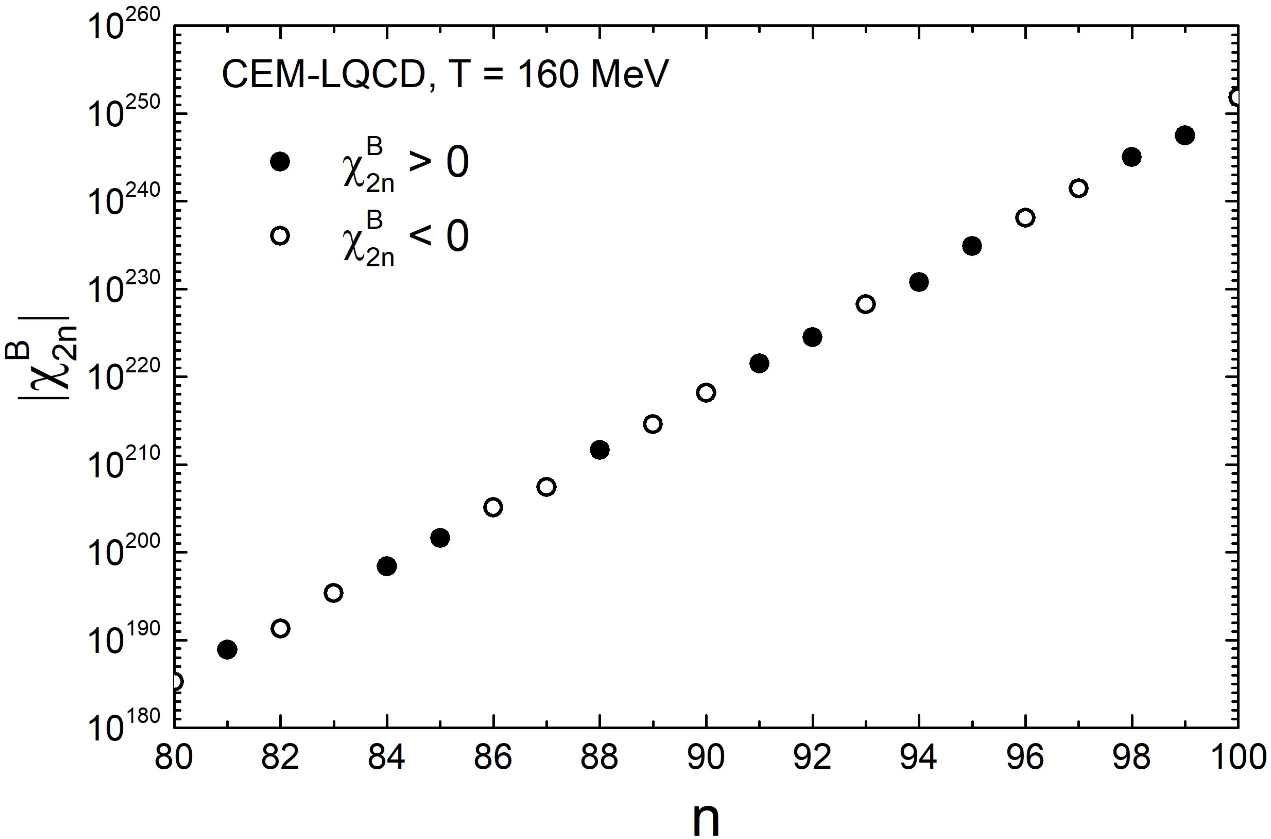

Negative coefficients appear eventually

They never settle into a regular (same- or alternate-sign) pattern

Using estimators for radius of convergence

a) Ratio estimator:

$$r_n = \left| \frac{(2n+2)(2n+1)\chi_{2n}^B}{\chi_{2n+2}^B} \right|^{1/2}$$

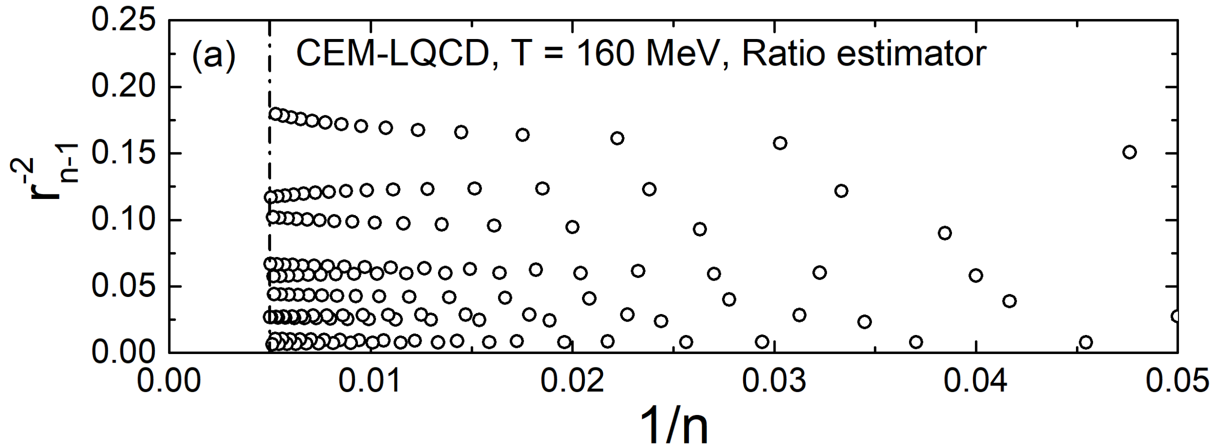

Ratio estimator is *unable* to determine the radius of convergence, nor to provide an upper or lower bound, *so use it with care!!*

b) Mercer-Roberts estim.:

$$r_n = \left| \frac{c_{n+1}\, c_{n-1} - c_n^2}{c_{n+2}\, c_n - c_{n+1}^2} \right|^{1/4}$$

$$c_n = \frac{\chi_{2n}^B}{(2n)!}$$

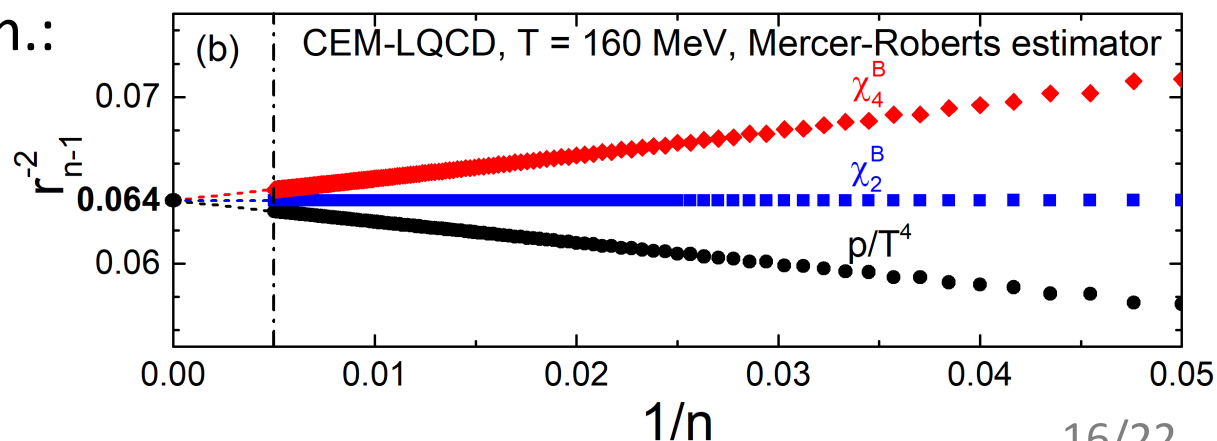

CEM: Radius of convergence

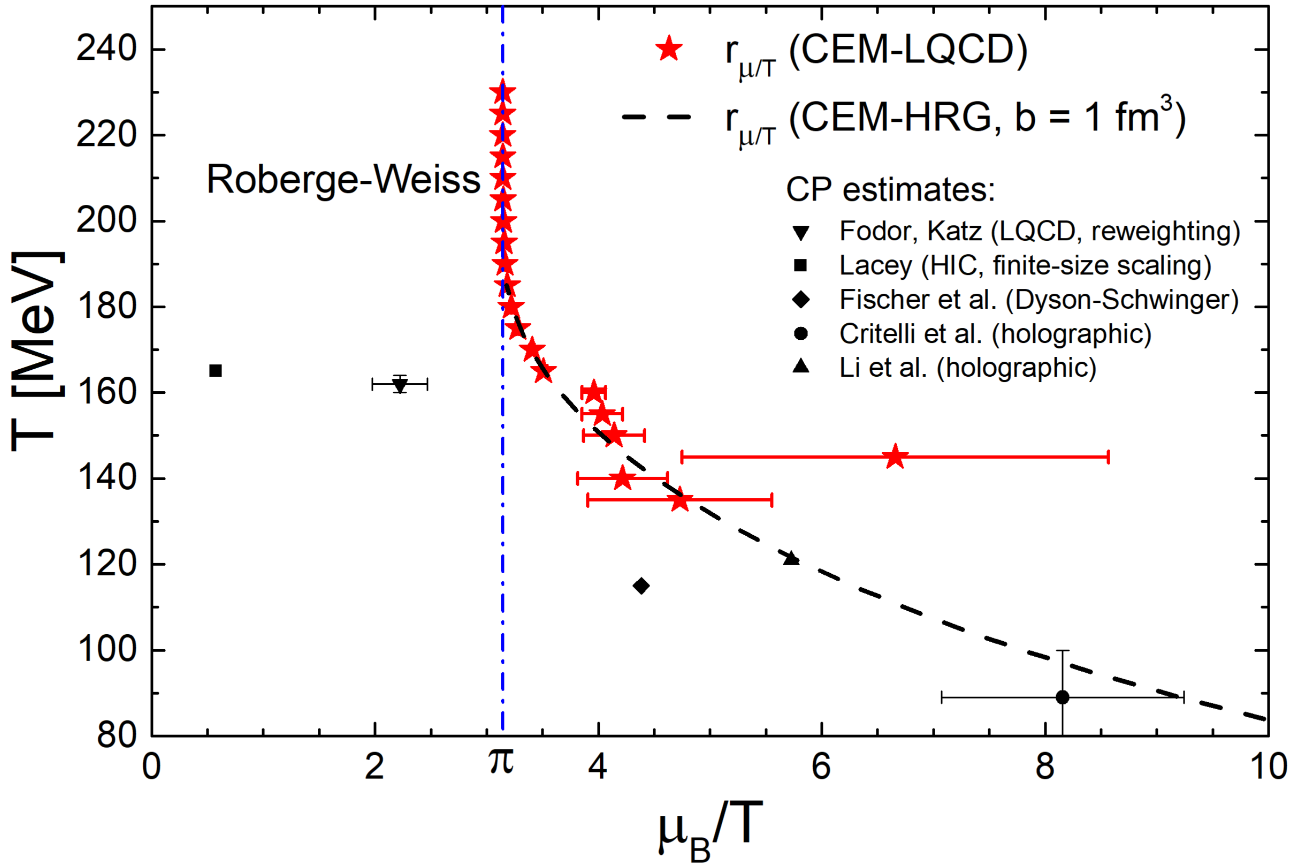

Radius of convergence approaches Roberge-Weiss transition value

- At $T > T_{RW}$ expected $\left[\frac{\mu_B}{T}\right]_c = \pm i\pi$ [Roberge, Weiss, NPB '86]
- Complex plane singularities interfere with the search for CP

$T_{RW} \sim 208$ MeV
[C. Bonati et al., 1602.01426]

Extracting $b_1(T)$ and $b_2(T)$ from susceptibilities

CEM: All χ_k^B determined by b_1 and b_2 at a given temperature

Reverse prescription: Extract $b_1(T)$ and $b_2(T)$ from two independent (combinations of) χ_k^B, *assuming that CEM is valid*

Extracting $b_1(T)$ and $b_2(T)$ from susceptibilities

CEM: All χ_k^B determined by b_1 and b_2 at a given temperature

Reverse prescription: Extract $b_1(T)$ and $b_2(T)$ from two independent (combinations of) χ_k^B, *assuming that CEM is valid*

Example: $b_1(T)$, $b_2(T)$ from HotQCD data for χ_2^B and χ_4^B/χ_2^B at $\mu_B = 0$

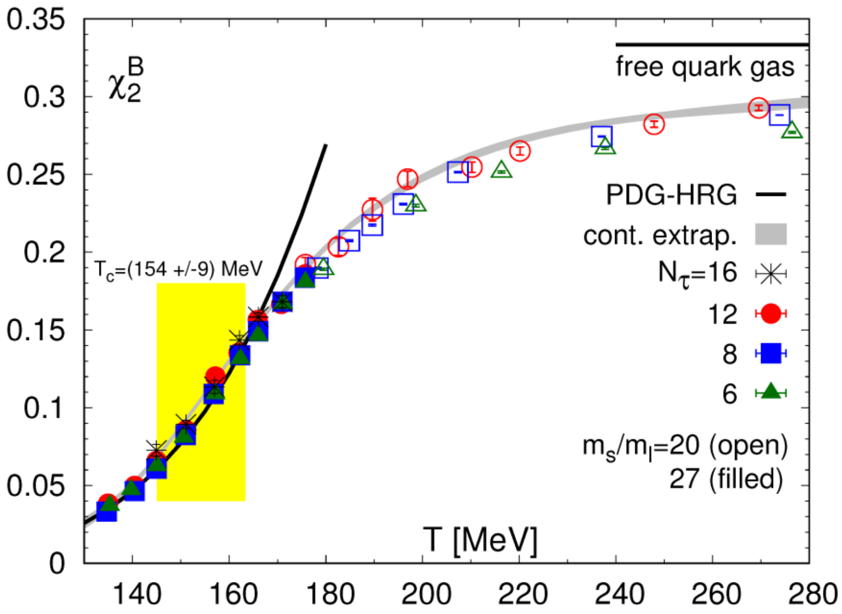

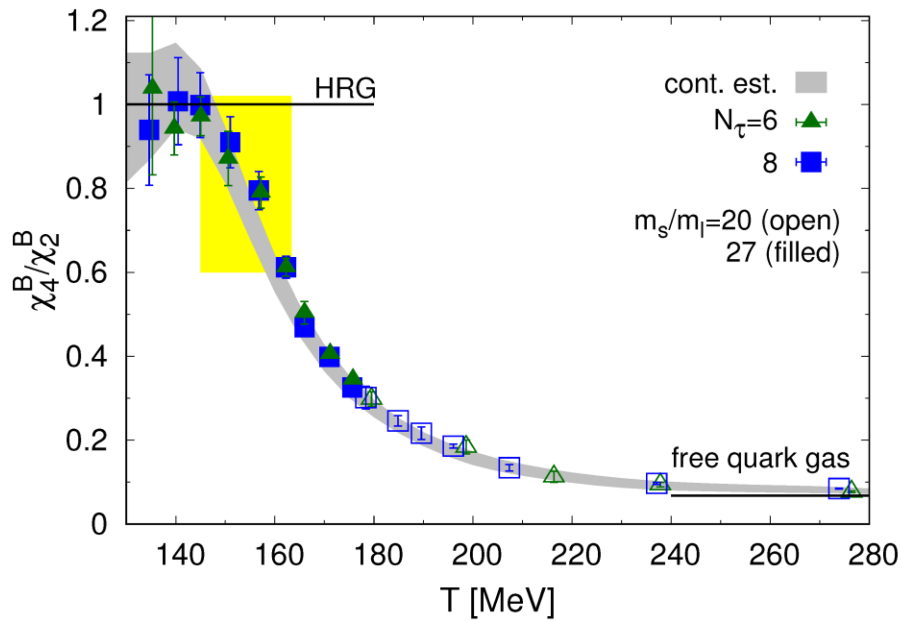

HotQCD collaboration, 1701.04325 & 1708.04897

Extracting $b_1(T)$ and $b_2(T)$ from susceptibilities

CEM: All χ_k^B determined by b_1 and b_2 at a given temperature

Reverse prescription: Extract $b_1(T)$ and $b_2(T)$ from two independent (combinations of) χ_k^B, *assuming that CEM is valid*

Example: $b_1(T)$, $b_2(T)$ from HotQCD data for χ_2^B and χ_4^B/χ_2^B at $\mu_B = 0$

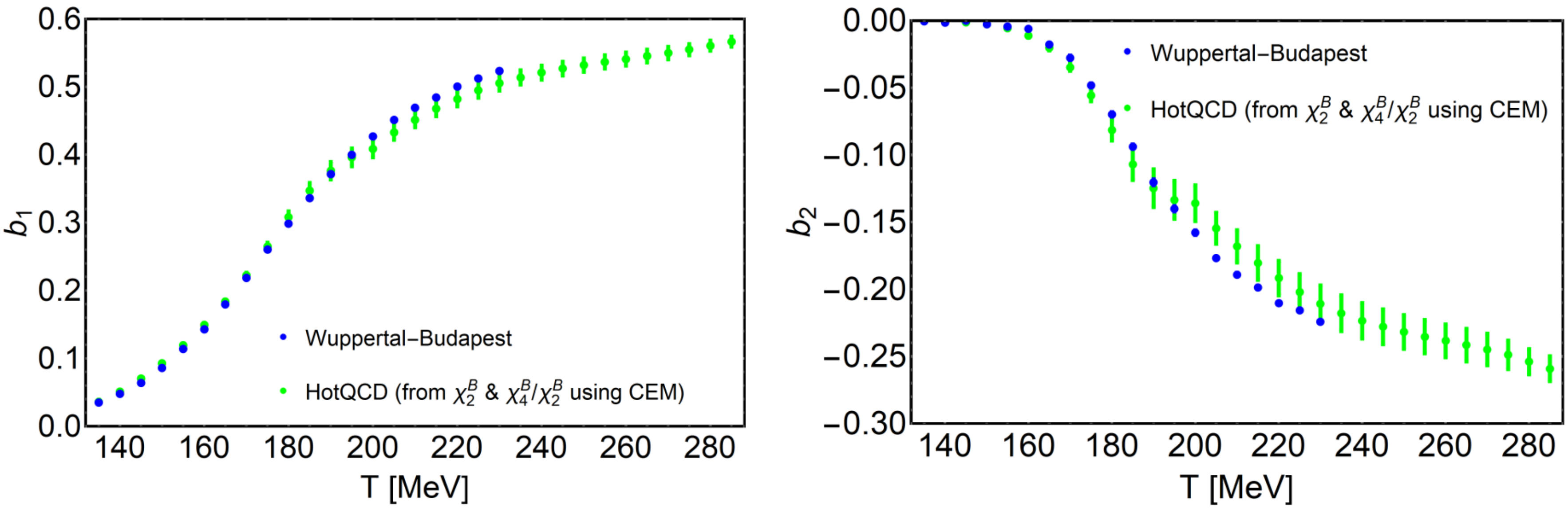

Implies accuracy of CEM and consistency between LQCD data of different groups

CEM: Reconstructing the full equation of state

Integrating the baryon number density

$$\frac{\rho_B}{T^3} = -\frac{2}{27\pi^2}\frac{\hat{b}_1^2}{\hat{b}_2}\left\{4\pi^2\left[\mathrm{Li}_1(x_+) - \mathrm{Li}_1(x_-)\right] + 3\left[\mathrm{Li}_3(x_+) - \mathrm{Li}_3(x_-)\right]\right\}$$

one obtains the scaled pressure $p(T,\mu_B)/T^4$ in CEM

$$\frac{p(T,\mu_B)}{T^4} = p_0(T) - \frac{2}{27\pi^2}\frac{\hat{b}_1^2}{\hat{b}_2}\left\{4\,\pi^2\left[\mathrm{Li}_2(x_+) + \mathrm{Li}_2(x_-)\right] + 3\left[\mathrm{Li}_4(x_+) + \mathrm{Li}_4(x_-)\right]\right\}$$

which provides the full equation of state within the model

Full model input:

- Fourier coefficients $b_1(T)$ and $b_2(T)$ $\leftarrow$ LQCD at imaginary μ_B
- μ_B-independent part of pressure $p_0(T)$ $\leftarrow$ LQCD EoS at $\mu_B = 0$

Useful for hydro at finite baryon density

CEM: Input parametrization

$$b_{1,2}^{lqcd}(T) = \frac{b_{1,2}^{sb} + \frac{a_{1,2}^{n}}{t} + \frac{b_{1,2}^{n}}{t^2}}{1 + \frac{a_{1,2}^{d}}{t} + \frac{b_{1,2}^{d}}{t^2}}, \quad t = \frac{T}{T_0}$$

Fit to WB lattice data,
T > 135 MeV [1708.02852]

$$\frac{p^{lqcd}(T, \mu_B = 0)}{T^4}$$

Parametrization from HotQCD collab. [1407.6387] $\rightarrow$ $p_0^{lqcd}(T)$

At lower temperatures matched with excluded-volume HRG model via the "switching function" [Albright, Kapusta, Young, 1404.7540]

$$b_{1,2}^{full}(T) = [1 - S(T)]\, b_{1,2}^{evhrg}(T) + S(T)\, b_{1,2}^{lqcd}(T)$$

$$S(T) = \mathrm{Exp}\left[-\left(\frac{T_{sw}}{T}\right)^r\right], \quad T_{sw} \approx 160 \text{ MeV}, \quad \mathrm{r} \approx 8$$

CEM: Isentropes

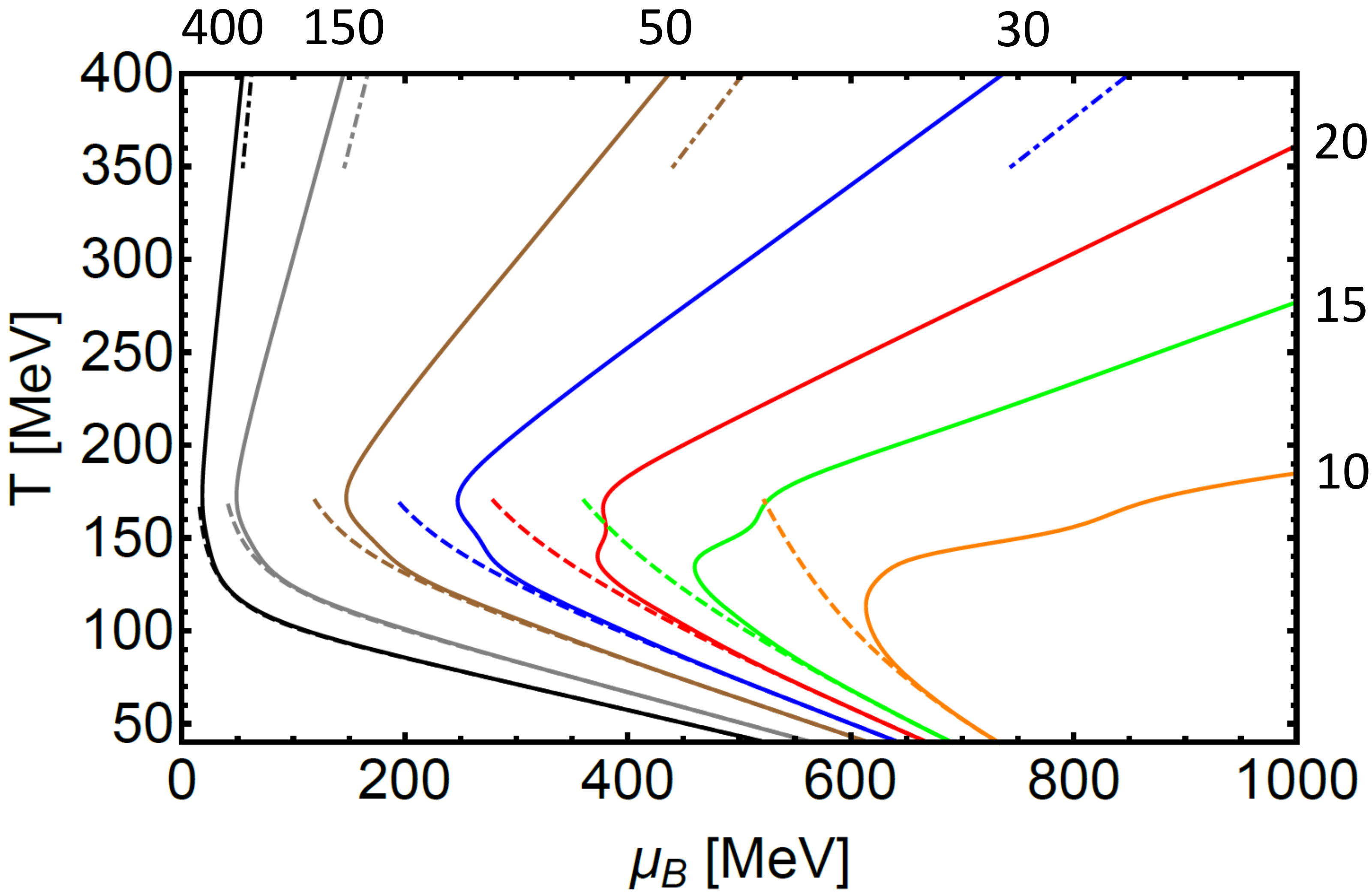

Implemented in hybrid UrQMD, work-in-progress

Summary

- Lattice QCD data at imaginary μ_B and $\mu_B = 0$ constrain strongly phenomenological models

- Initial deviations from the uncorrelated gas of hadrons can be understood in terms of repulsive baryonic interactions

- Cluster expansion model (CEM) is consistent with presently available lattice data, both at $\mu = 0$ and imaginary μ_B. Model has no singularities at real μ_B $\rightarrow$ *no unambiguous signal of CP*

- CEM equation of state is suitable for hydro simulations of heavy-ion collisions at finite baryon density

Summary

- Lattice QCD data at imaginary μ_B and $\mu_B = 0$ constrain strongly phenomenological models
- Initial deviations from the uncorrelated gas of hadrons can be understood in terms of repulsive baryonic interactions
- Cluster expansion model (CEM) is consistent with presently available lattice data, both at $\mu = 0$ and imaginary μ_B. Model has no singularities at real μ_B $\rightarrow$ *no unambiguous signal of CP*
- CEM equation of state is suitable for hydro simulations of heavy-ion collisions at finite baryon density

Thanks for your attention!

Backup slides

Expected asymptotics

- At low T/densities QCD $\simeq$ ideal hadron resonance gas

$$\frac{p^{\rm hrg}(T,\mu_B)}{T^4} = \frac{\phi_M(T)}{T^3} + 2\,\frac{\phi_B(T)}{T^3}\cosh\left(\frac{\mu_B}{T}\right),$$

$$\phi_B(T) = \sum_{i\in B}\int dm\,\rho_i(m)\,\frac{d_i\,m^2\,T}{2\pi^2}\,K_2\left(\frac{m}{T}\right),$$

$$p_0^{hrg}(T) = \frac{\phi_M(T)}{T^3}, \quad p_1^{hrg}(T) = \frac{2\,\phi_B(T)}{T^3}, \quad p_k^{\rm hrg}(T) \equiv 0,\ k \geq 2$$

- At high T QCD $\simeq$ ideal gas of massless quarks and gluons

$$\frac{p^{\rm SB}(T,\mu_B)}{T^4} = \frac{8\pi^2}{45} + \sum_{f=u,d,s}\left[\frac{7\pi^2}{60} + \frac{1}{2}\left(\frac{\mu_B}{3T}\right)^2 + \frac{1}{4\pi^2}\left(\frac{\mu_B}{3T}\right)^4\right],$$

$$p_0^{\rm SB} = \frac{64\pi^2}{135}, \quad p_k^{\rm SB} = \frac{(-1)^{k+1}}{k^2}\,\frac{4\,[3+4\,(\pi k)^2]}{27\,(\pi k)^2}, \quad b_k^{SB} = k\,p_k^{\rm SB}.$$

Lattice data explore intermediate, transition region $130 < T < 230$ MeV

*In this study we assume that $\mu_S = \mu_Q = 0$

CEM: Baryon number fluctuations

Baryon number susceptibilities at $\mu_B = 0$:

$$\chi_{2n}^{B}(T) \equiv \left.\frac{\partial^{2n}(p/T^4)}{\partial(\mu_B/T)^{2n}}\right|_{\mu_B=0} = \sum_{k=1}^{\infty} k^{2n-1}\, b_k(T) \simeq \sum_{k=1}^{k_{\max}} k^{2n-1}\, b_k(T).$$

CEM-LQCD: $b_1(T)$ and $b_2(T)$ taken from LQCD simulations at imaginary μ_B

χ_2^B

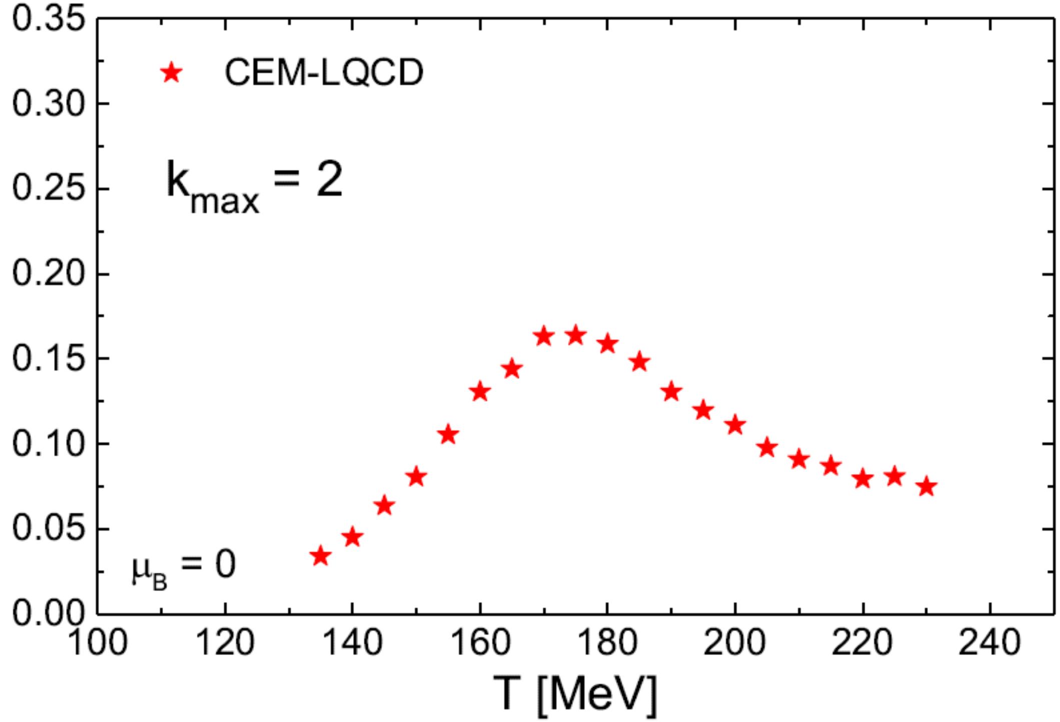

CEM: Higher-order susceptibilities

$$\chi_k^B(T,\mu_B) = -\frac{2}{27\pi^2}\frac{\hat{b}_1^2}{\hat{b}_2}\left\{4\pi^2\left[\mathrm{Li}_{2\text{-}k}(x_+) + (-1)^k\ \mathrm{Li}_{2\text{-}k}(x_-)\right] + 3\left[\mathrm{Li}_{4\text{-}k}(x_+) + (-1)^k\ \mathrm{Li}_{4\text{-}k}(x_-)\right]\right\}$$

χ_8^B

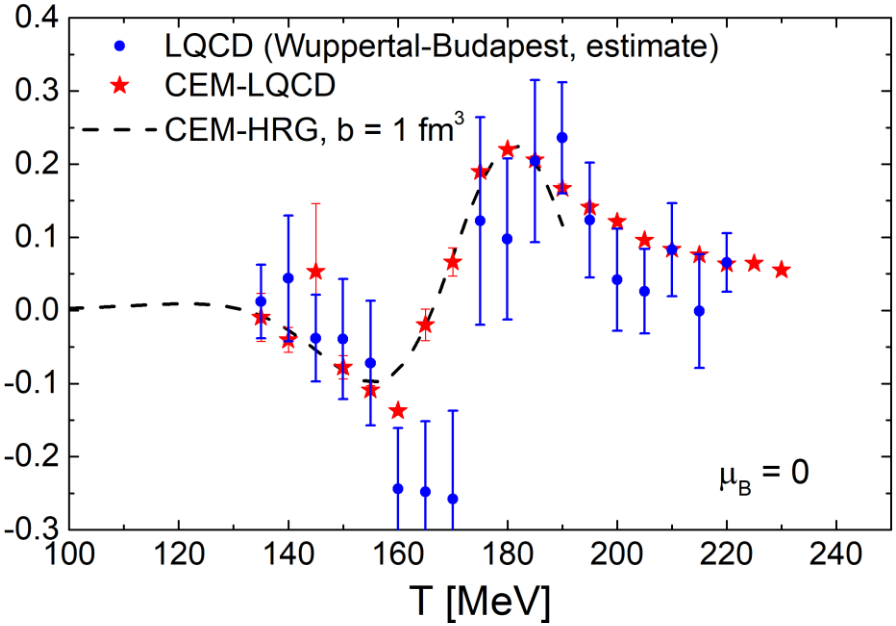

χ_{10}^B

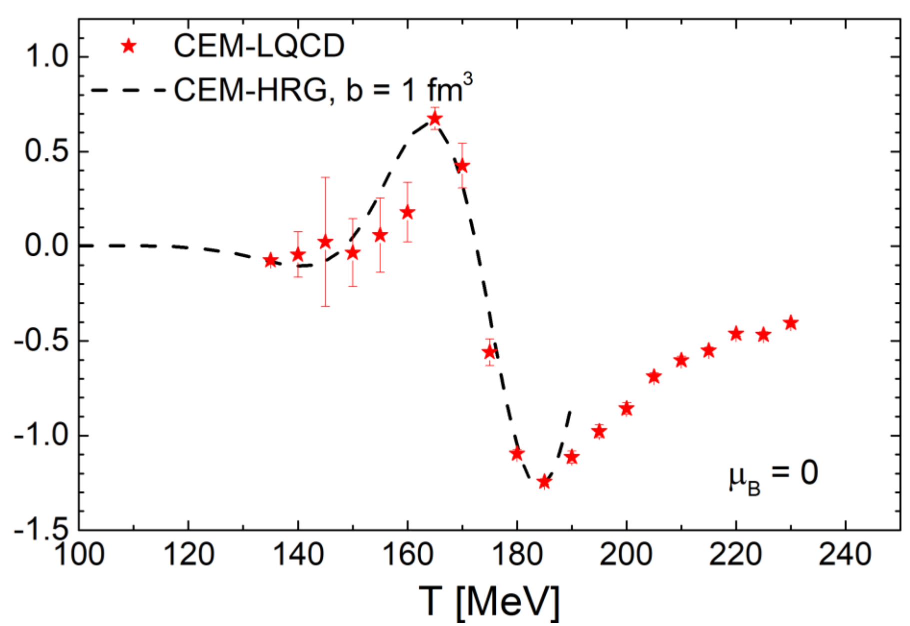

Preliminary lattice estimate from 1805.04445 (Wuppertal-Budapest)

To be verified by future lattice data

CEM: Observables at finite μ_B

χ_4^B/χ_2^B

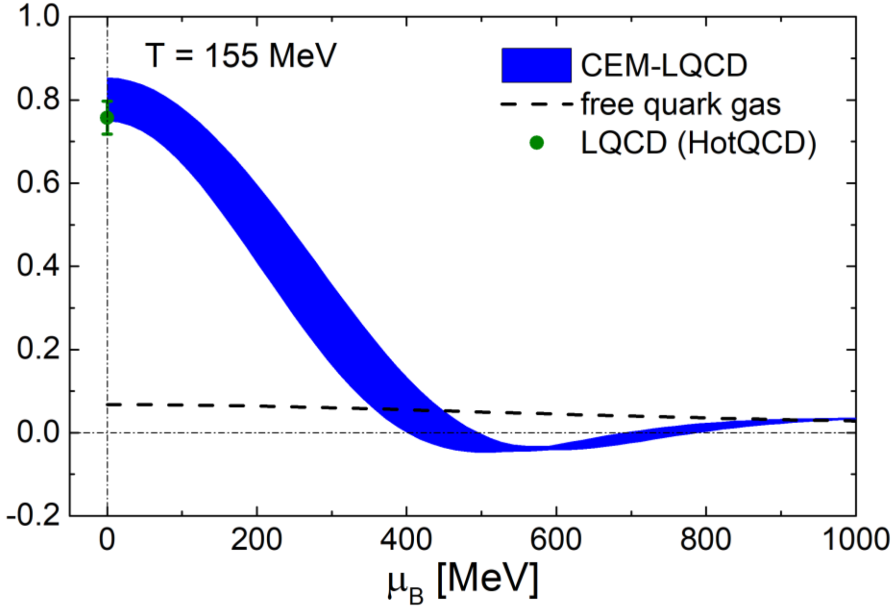

χ_6^B/χ_2^B

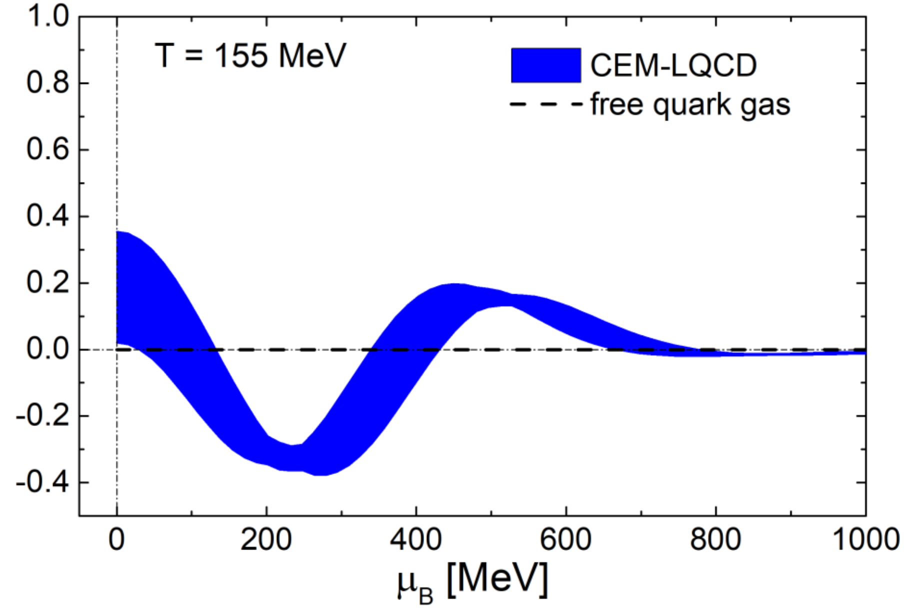

- Non-monotonic μ_B dependence of χ_4^B/χ_2^B and χ_6^B/χ_2^B
- Ratios consistent with free Fermi gas in the limit of large μ_B
- $\chi_6^B/\chi_2^B \lesssim 0$ in the STAR-BES range